Method for Calculating the Interlaminar Stresses in Symmetric Laminates Containing a Circular Hole

Chu-Cheng Ko* and Chien-Chang Lin†
National Chung-Hsing University, Taichung, Taiwan 40227, Republic of China

An efficient approximate solution for three-dimensional stress distributions around a circular hole in symmetric laminates under a set of far-field in-plane stresses is presented. Stress functions for each ply are assumed according to the boundary-layer equilibrium equations. In addition, all the boundary conditions for each ply and traction continuity at the ply interface are exactly satisfied. Eventually, the unknown parameters in stress functions are determined by the minimization of complementary energy of the whole laminate. Numerical examples are presented in comparison with given literature which shows that the present method is efficient.

I. Introduction

DUE to stiffness discontinuity between plies, it is easy to cause interlaminar stress concentrations near the free-edge region in composite laminates. Such stresses will commence delamination, matrix crackings, and failure of laminates, especially under fatigue loading.

Since 1970, numerous investigations[1-5] have used various methods to determine the interlaminar stresses at the straight free edge of composite laminates. Pipes and Pagano[1] adopted the anisotropic elasticity theory in conjunction with the finite difference method to analyze a simple four-ply laminate. Wang and Crossman[2] used a finite element approach to investigate this same problem. Wang and Choi[3,4] derived an analytical solution based on Lekhnitskii's stress potentials and the theory of anisotropic elasticity to determine the exact order of stress singularity at the free edges of laminate. In an effort to develop an efficient method to deal with thick laminates (say 100 plies), Kassapoglou and Lagace[5] used the force balance method in conjunction with the principle of minimum complementary energy to obtain an analytical solution for interlaminar stresses at straight free edges.

Owing to the complicated geometry for the curved free edges as compared with the straight free edges, little work has been done for composite laminates with curved free edges. Basically, the analysis of straight free edge may be assumed as a problem with two-dimensional stress and strain variations. However, the curved free edge is a typical three-dimensional problem. This difference has rendered the analysis for the curved free edge more difficult than the straight free edge. A boundary-layer theory based on the perturbation technique for isotropic elastic plates with a circular hole developed by Reiss[6] has been extended to composite laminates by Tang.[7,8] This approach is based on identifying the boundary-layer problem as two equivalent problems, namely, a modified torsion problem and a modified plane strain problem. However, Tang's solution can only satisfy part of boundary conditions in an average sense, which may result in unreliable stress results near the free edges.[9] In addition, Tang's solution will be very tedious for laminates with numerous plies. Zhang and Ueng[10] proposed a simplified method to investigate the effect of the ratio of hole radius to laminate thickness on the interlaminar stress distributions around a hole in a $(0/90\ \text{deg})_S$ laminate under far-field tensile or shear stress; however, it is assumed that the order of stress singularity is prescribed and independent of the material properties and ply orientations of the laminate.

Numerical investigations such as finite element methods have also been used to analyze the interlaminar stress distributions around the curve free edge. Rybicki and Schmuesser[11] used a structural analysis package SAP IV and adopted a common three-dimensional isoparametric, compatible displacement element to model each ply in the laminate. Problems were selected to evaluate the effect of stacking sequence and lay-up angle on the interlaminar normal stress distributions around the hole. Similarly, Lucking et al.[12] also used the SAP IV program to investigate the effect of hole-radius-to-laminate-thickness ratio on the interlaminar stress distributions around the hole in a $(0/90\ \text{deg})_S$ laminate. The results of these two studies are based on the conventional displacement finite element method so that compatability is exactly satisfied while the equilibrium equations and free-edge boundary conditions are only approximately satisfied. This drawback may lead to questionable stress results near the free edge, which has been strongly emphasized by Spilker and Chou.[9] Rybicki and Hopper[13] derived an equilibrium stress field from Maxwell stress functions that are continuous even along the ply interface. However, this assumption violates the fact that the in-plane stresses are only piecewise continuous through the laminate thickness. Nishioka and Atluri[15] developed a "special-hole-element" which was based on a modified complementary energy principle and the embedded analytical asymptotic stress solution near the hole. Bar-Yoseph and Avrashi[16] extended the boundary-layer theory in conjunction with a variational-perturbation technique and assumed stress finite element method for the analysis of three-dimensional stress distributions around a curvilinear hole in laminates. One of the shortcomings associated with the above finite difference, finite element, stress potentials, and boundary-layer theory solutions is that they may be inefficient or tedious for laminates with numerous plies. Such limitations make it hard to handle thick laminates. So far, to the authors' knowledge, Pagano and Soni[17] developed a global-local model that could handle laminates with numerous plies. However, the solution is very sensitive to the substructuring technique.

The main purpose of the present work is to establish an efficient method of analyzing the interlaminar stress distributions around a circular hole in symmetric laminates under a set of far-field in-plane stresses. This method takes the advantage of Kassapoglou and Lagace's technique[5] for the straight free edge in conjunction with the boundary-layer theory. All the boundary conditions for each ply and interface traction continuity are exactly satisfied. Comparisons of the present results with the available data in literature demonstrates the efficiency and accuracy of this method.

Received Aug. 17, 1990; revision received April 29, 1991; accepted for publication April 29, 1991.

*Graduate Student, Institute of Applied Mathematics.
†Professor, Institute of Applied Mathematics. Member AIAA.

II. Method of Stress Analysis

Consider a symmetric laminate with N orthotropic piles of equal thickness t. The laminate has a circular hole of radius R and is subjected to a set of far-field in-plane stresses as shown in Fig. 1. The origin point of the local coordinate is located at the center of the hole on the bottom surface of each ply.

The equilibrium equations, in the absence of body forces, can be written in a polar coordinate system

$$\frac{\partial \sigma_{rr}^{(k)}}{\partial r} + \frac{1}{r}\frac{\partial \tau_{r\theta}^{(k)}}{\partial \theta} + \frac{\partial \tau_{rz}^{(k)}}{\partial z} + \frac{\sigma_{rr}^{(k)} - \sigma_{\theta\theta}^{(k)}}{r} = 0$$

$$\frac{\partial \tau_{r\theta}^{(k)}}{\partial r} + \frac{1}{r}\frac{\partial \sigma_{\theta\theta}^{(k)}}{\partial \theta} + \frac{\partial \tau_{z\theta}^{(k)}}{\partial z} + \frac{2\tau_{r\theta}^{(k)}}{r} = 0$$

$$\frac{\partial \tau_{rz}^{(k)}}{\partial r} + \frac{1}{r}\frac{\partial \tau_{z\theta}^{(k)}}{\partial \theta} + \frac{\partial \sigma_{zz}^{(k)}}{\partial z} + \frac{\tau_{rz}^{(k)}}{r} = 0 \qquad (1)$$

where $\sigma_{rr}^{(k)}$, $\sigma_{\theta\theta}^{(k)}$, $\sigma_{zz}^{(k)}$ are normal stress components and $\tau_{r\theta}^{(k)}$, $\tau_{rz}^{(k)}$, $\tau_{z\theta}^{(k)}$ are shear stress components of the kth ply in terms of polar coordinates.

Analogous to Refs. 6 and 7, the following nondimensional variables are defined:

$$\xi = (r - R)/R, \quad \xi \geq 0; \qquad \rho = z^{(k)}/t, \quad 0 \leq \rho \leq 1$$

$$\varepsilon = t/R; \qquad \eta = \xi/\varepsilon$$

The equilibrium equations for the kth ply can be modified as Eq. (2), and the senses of positive stresses are shown in Fig. 2:

$$\tau_{rz,\rho}^{(k)} + \varepsilon\left[\sigma_{rr,\xi}^{(k)} + \frac{1}{1+\xi}(\tau_{r\theta,\theta}^{(k)} + \sigma_{rr}^{(k)} - \sigma_{\theta\theta}^{(k)})\right] = 0$$

$$\tau_{z\theta,\rho}^{(k)} + \varepsilon\left[\tau_{r\theta,\xi}^{(k)} + \frac{1}{1+\xi}(\sigma_{\theta\theta,\theta}^{(k)} + 2\tau_{r\theta}^{(k)})\right] = 0$$

$$\sigma_{zz,\rho}^{(k)} + \varepsilon\left[\tau_{rz,\xi}^{(k)} + \frac{1}{1+\xi}(\tau_{z\theta,\theta}^{(k)} + \tau_{rz}^{(k)})\right] = 0 \qquad (2)$$

Now, the region under consideration is divided into interior region and boundary-layer region and each stress component is to be determined by superposition of the interior stress σ_{ij}^{o} and boundary-layer stress f_{ij}. In the interior region, Lekhnitskii's theory of two-dimensional anisotropic elasticity[18] in conjunction with classical lamination plate theory[19] is adopted. In the vicinity of free edge around the hole, namely, the boundary-layer region, there exists a three-dimensional stress state of each ply, and the above two-dimensional anisotropic elasticity is inadequate.

The equilibrium equations in the boundary-layer region may be approximated by expressing the boundary-layer stress components f_{ij} as the perturbation series of ε:

$$f_{ij}(\eta, \theta, \rho, \varepsilon) = \sum_{n=0}^{\infty} f_{ij}^{(n)}(\eta, \theta, \rho)\varepsilon^n \qquad (3)$$

where $f_{ij}^{(n)} = 0$ for $n < 0$.

Introducing Eq. (3) into Eq. (2) and equating like powers of ε, we obtain a series of differential equations for the boundary layer. The zeroth-order approximation is given by the solution of the following equilibrium equations:

$$f_{rz,\rho}^{0(k)} + f_{rr,\eta}^{0(k)} = 0$$

$$f_{z\theta,\rho}^{0(k)} + f_{r\theta,\eta}^{0(k)} = 0$$

$$f_{zz,\rho}^{0(k)} + f_{rz,\eta}^{0(k)} = 0 \qquad (4)$$

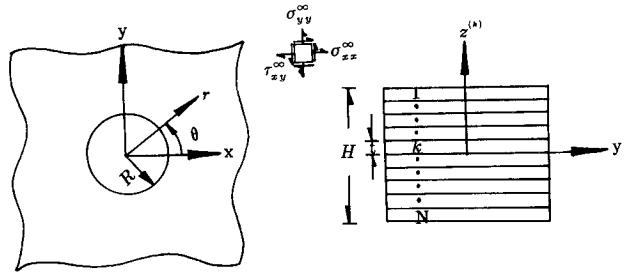

Fig. 1 Laminate geometry and coordinate system.

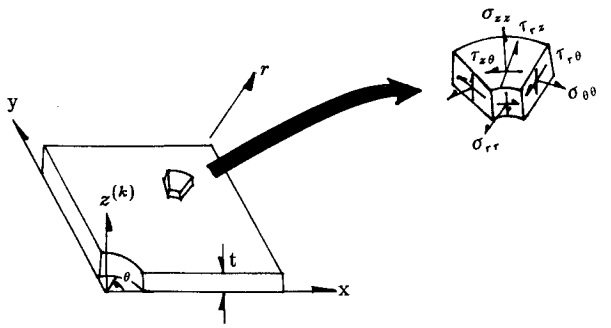

Fig. 2 Senses of positive stresses.

It can be seen that equilibrium equations of the zeroth-order approximation are much simplier than the original equilibrium equations (2). In addition, the circumferential stress component $f_{\theta\theta}^{0(k)}$ has been dropped in the zeroth-order equilibrium equations.

The first-order approximation requires a solution of the differential equations

$$f_{rz,\rho}^{1(k)} + f_{rr,\eta}^{1(k)} + \eta f_{rz,\rho}^{0(k)} + \eta f_{rr,\eta}^{0(k)} + f_{r\theta,\theta}^{0(k)} + f_{rr}^{0(k)} - f_{\theta\theta}^{0(k)} = 0$$

$$f_{z\theta,\rho}^{1(k)} + f_{r\theta,\eta}^{1(k)} + \eta f_{z\theta,\rho}^{0(k)} + \eta f_{r\theta,\eta}^{0(k)} + f_{\theta\theta,\theta}^{0(k)} + 2f_{r\theta}^{0(k)} = 0$$

$$f_{zz,\rho}^{1(k)} + f_{rz,\eta}^{1(k)} + \eta f_{zz,\rho}^{0(k)} + \eta f_{rz,\eta}^{0(k)} + f_{z\theta,\theta}^{0(k)} + f_{rz}^{0(k)} = 0 \qquad (5)$$

The high-order approximations can be obtained similarly.

In this study, we have restricted our attention to the zeroth-order approximation, and the approximate stess solutions for the boundary-layer region can be obtained according to the following procedures:

1) Select the appropriate stress functions that satisfy the equilibrium equations.

2) Determine the coefficients of the stress functions by satisfying the associated boundary conditions and interface traction continuity.

3) Minimize the complementary energy to determine the remaining unknown parameters.

A. Stress Functions for Boundary-Layer Region

In order to seek the stress solutions for the boundary-layer region, we may assume that each stress component (except for $f_{\theta\theta}^{0(k)}$), for the kth ply, can be expressed as the product of two independent functions, such that

$$f_{ij}^{0(k)} = g_{ij}^{(k)}(\rho)h_{ij}^{(k)}(\eta) \qquad (6)$$

here, functions $g_{ij}^{(k)}(\rho)$, $h_{ij}^{(k)}(\eta)$ are to be determined for each ply in the laminate.

On substitution of Eq. (6) into equilibrium equation (4), we can find that the unknown functions are related as follows:

$$\frac{dg_{rz}^{(k)}}{d\rho} = g_{rr}^{(k)} \tag{7a}$$

$$\frac{dg_{zz}^{(k)}}{d\rho} = g_{rz}^{(k)} \tag{7b}$$

$$\frac{dg_{z\theta}^{(k)}}{d\rho} = g_{r\theta}^{(k)} \tag{7c}$$

$$-\frac{dh_{rr}^{(k)}}{d\eta} = h_{rz}^{(k)} \tag{8a}$$

$$-\frac{dh_{rz}^{(k)}}{d\eta} = h_{zz}^{(k)} \tag{8b}$$

$$-\frac{dh_{r\theta}^{(k)}}{d\eta} = h_{z\theta}^{(k)} \tag{8c}$$

It can be observed that the required minimum number of the unknown functions $g_{ij}^{(k)}(\rho)$, $h_{ij}^{(k)}(\eta)$ is four in each ply. Once these four functions are determined, the remaining functions can be obtained by Eqs. (7a–7c) and (8a–8c).

In view of Eqs. (7a–7c), we may select $g_{rr}^{(k)}$ and $g_{r\theta}^{(k)}$ as our basic approximate functions of ρ, and assume

$$g_{rr}^{(k)} = B_1^{(k)} \tag{9a}$$

$$g_{r\theta}^{(k)} = B_4^{(k)} \tag{9b}$$

The substitution of Eqs. (9a) and (9b) into Eqs. (7a–7c), and integration with respect to ρ yield the remaining expressions for $g_{ij}^{(k)}(\rho)$ in the kth ply as follows:

$$g_{rz}^{(k)} = B_1^{(k)}\rho + B_2^{(k)} \tag{9c}$$

$$g_{zz}^{(k)} = \tfrac{1}{2}B_1^{(k)}\rho^2 + B_2^{(k)}\rho + B_3^{(k)} \tag{9d}$$

$$g_{z\theta}^{(k)} = B_4^{(k)}\rho + B_5^{(k)} \tag{9e}$$

In the present application, it is considered for simplicity that $B_1^{(k)}$ and $B_4^{(k)}$ are fixed as unity with no loss of generality.

Similarly, we select $h_{rr}^{(k)}$ and $h_{r\theta}^{(k)}$ as our basic approximate functions of η, and assume

$$h_{rr}^{(k)} = A_1^{(k)} \exp(-\lambda_1\eta) + A_2^{(k)} \exp(-\lambda_1\lambda_2\eta) \tag{10a}$$

$$h_{r\theta}^{(k)} = A_3^{(k)} \exp(-\lambda_1\eta) \tag{10b}$$

Here, λ_1 and λ_2 may be regarded as decay parameters.

Putting Eqs. (10a) and (10b) into Eqs. (8a–8c) and taking differentiations with respect to η, the remaining expressions for $h_{ij}^{(k)}(\eta)$ in the kth ply can be obtained:

$$h_{rz}^{(k)} = A_1^{(k)}\lambda_1 \exp(-\lambda_1\eta) + A_2^{(k)}\lambda_1\lambda_2 \exp(-\lambda_1\lambda_2\eta) \tag{10c}$$

$$H_{zz}^{(k)} = A_1^{(k)}\lambda_1^2 \exp(-\lambda_1\eta) + A_2^{(k)}\lambda_1^2\lambda_2^2 \exp(-\lambda_1\lambda_2\eta) \tag{10d}$$

$$h_{z\theta}^{(k)} = A_3^{(k)}\lambda_1 \exp(-\lambda_1\eta) \tag{10e}$$

In the above stress expressions, the coefficients $A_i^{(k)}$ and $B_i^{(k)}$ are to be determined by the associated boundary conditions and interface traction continuity. In addition, circumferential stress function $f_{\theta\theta}^{0(k)}$, which has been dropped in the zeroth-order approximation, can be obtained by setting the boundary-layer circumferential strain $\varepsilon_{\theta\theta}^{0(k)}$ to be zero.[7]

B. Boundary Conditions and Interface Traction Continuity

The associated boundary conditions and interface traction continuity by the zeroth-order approximation can be given as follows:

1) At infinity, boundary-layer stress components $f_{ij}^{0(k)}$ will vanish and boundary conditions will be satisfied by the interior region in a stress resultant concept

$$\lim_{\eta\to\infty} \{f_{rr}^{0(k)}, f_{r\theta}^{0(k)}, f_{rz}^{0(k)}, f_{z\theta}^{0(k)}, f_{zz}^{0(k)}\} = 0$$

$$k = 1, 2, \ldots, N \tag{11a}$$

2) On the top and bottom surface of the laminate

$$f_{rz}^{0(k)} = f_{z\theta}^{0(k)} = f_{zz}^{0(k)} = 0 \tag{11b}$$

3) At the interface of two adjacent plies

$$f_{rz}^{0(k)} = f_{rz}^{0(k+1)}$$

$$f_{z\theta}^{0(k)} = f_{z\theta}^{0(k+1)}$$

$$f_{zz}^{0(k)} = f_{zz}^{0(k+1)}, \qquad k = 1, 2, \ldots, N-1 \tag{11c}$$

4) Along the hole boundary, i.e., $\eta = 0$

$$\sigma_{rr}^{(k)} = f_{rr}^{0(k)} + \sigma_{rr}^{0(k)} = 0$$

$$\tau_{r\theta}^{(k)} = f_{r\theta}^{0(k)} + \tau_{r\theta}^{0(k)} = 0$$

$$f_{rz}^{0(k)} = 0, \qquad k = 1, 2, \ldots, N \tag{11d}$$

C. Stress Solutions for Interior Region

According to Lekhnitskii's theory of two-dimensional anisotropic elasticity,[18] stress solutions near a hole resulting from a set of far-field stresses σ_{xx}^{∞}, σ_{yy}^{∞}, τ_{xy}^{∞} can be given as follows:

$$\begin{aligned}
\sigma_{rr}^{0} &= 2Re[(\sin\theta - \mu_1\cos\theta)^2\Phi_1' \\
&\quad + (\sin\theta - \mu_2\cos\theta)^2\Phi_2'] \\
&\quad + \sigma_{xx}^{\infty}\cos^2\theta + \sigma_{yy}^{\infty}\sin^2\theta + 2\tau_{xy}^{\infty}\sin\theta\cos\theta \\
\sigma_{\theta\theta}^{0} &= 2Re[(\cos\theta + \mu_1\sin\theta)^2\Phi_1' \\
&\quad + (\cos\theta + \mu_2\sin\theta)^2\Phi_2'] \\
&\quad + \sigma_{xx}^{\infty}\sin^2\theta + \sigma_{yy}^{\infty}\cos^2\theta - 2\tau_{xy}^{\infty}\sin\theta\cos\theta \\
\tau_{r\theta}^{0} &= 2Re[(\sin\theta - \mu_1\cos\theta)(\cos\theta + \mu_1\sin\theta)\Phi_1' \\
&\quad + (\sin\theta - \mu_2\cos\theta)(\cos\theta + \mu_2\sin\theta)\Phi_2'] \\
&\quad + (\sigma_{yy}^{\infty} - \sigma_{xx}^{\infty})\sin\theta\cos\theta + \tau_{xy}^{\infty}(\cos^2\theta - \sin^2\theta)
\end{aligned} \tag{12}$$

in which

$$\Phi_1' = \frac{-i}{2(\mu_1 - \mu_2)(1 + i\mu_1)}\{\sigma_{xx}^{\infty} + \sigma_{yy}^{\infty}i\mu_2 + \tau_{xy}^{\infty}(i + \mu_2)\} \times \left\{1 - \frac{r(\cos\theta + \mu_1\sin\theta)}{\sqrt{r^2(\cos\theta + \mu_1\sin\theta)^2 - R^2(1 + \mu_1^2)}}\right\}$$

$$\Phi_2' = \frac{i}{2(\mu_1 - \mu_2)(1 + i\mu_2)}\{\sigma_{xx}^{\infty} + \sigma_{yy}^{\infty}i\mu_1 + \tau_{xy}^{\infty}(i + \mu_1)\} \times \left\{1 - \frac{r(\cos\theta + \mu_2\sin\theta)}{\sqrt{r^2(\cos\theta + \mu_2\sin\theta)^2 - R^2(1 + \mu_2^2)}}\right\}$$

and $i = \sqrt{-1}$, and μ_1 and μ_2 are the complex roots obtained from the characteristic equation.[18]

Using the classical lamination plate theory and coordinate transformations, the in-plane stress components for the kth ply can be obtained in the following matrix form:

$$\begin{Bmatrix} \sigma^0_{rr} \\ \sigma^0_{\theta\theta} \\ \tau^0_{r\theta} \end{Bmatrix}^{(k)} = \begin{bmatrix} a_{11} & a_{12} & a_{13} \\ a_{21} & a_{22} & a_{23} \\ a_{31} & a_{32} & a_{33} \end{bmatrix}^{(k)} \begin{Bmatrix} \sigma^0_{rr} \\ \sigma^0_{\theta\theta} \\ \tau^0_{r\theta} \end{Bmatrix} \tag{13}$$

and

$$[a]^{(k)} = [T][\bar{Q}]^{(k)}[b][T]^{-1}$$

wherein $[T]$ is the coordinate transformation matrix, $[\bar{Q}]^{(k)}$ is the transformed stiffness matrix of the kth ply in xy coordinates, and $[b]$ is the laminate-equivalent anisotropic compliance matrix.

D. Stress Solutions for Boundary-Layer Region

From the assumed stress functions, Eqs. (9) and (10), in conjunction with associated boundary conditions, Eqs. (11a) and (11d), we have

$$\begin{aligned} A_1^{(k)} &= -A_2^{(k)}\lambda_2 = -\frac{\lambda_2}{\lambda_2 - 1} a_{12}^{(k)} \sigma^0_{\theta\theta}|_{\eta=0} \\ A_2^{(k)} &= \frac{a_{12}^{(k)}}{\lambda_2 - 1} \sigma^0_{\theta\theta}|_{\eta=0} \\ A_3^{(k)} &= -a_{32}^{(k)} \sigma^0_{\theta\theta}|_{\eta=0} \end{aligned} \tag{14}$$

here

$$\begin{aligned} \sigma^0_{\theta\theta}|_{\eta=0} = \frac{E_\theta}{E_x} \{ & \sigma^\infty_{xx}[-k\cos^2\theta + (1+n)\sin^2\theta] \\ & + \sigma^\infty_{yy}[k(k+n)\cos^2\theta - k\sin^2\theta] \\ & - \tau^\infty_{xy}[n(1+k+n)\sin\theta\cos\theta] \} \end{aligned}$$

and

$$\frac{E_\theta}{E_x} = \frac{1}{\sin^4\theta + (n^2 - 2k)\sin^2\theta\cos^2\theta + k^2\cos^4\theta}$$

$$k = \sqrt{\frac{E_x}{E_y}}, \quad m = \frac{E_x}{G_{xy}} - 2\nu_{xy}, \quad n = \sqrt{2k + m}$$

wherein E_x, E_y, G_{xy}, and ν_{xy} are the laminate-equivalent moduli in xy coordinates.

Next, from the interface traction continuity conditions, Eq. (11c), and traction-free conditions at the top and bottom surface of the laminate, Eq. (11b), we have

$$\begin{aligned} B_1^{(k)} &= 1 \\ B_2^{(k)} &= \frac{1}{a_{12}^{(k)}} \sum_{j=k+1}^{N} a_{12}^{(j)} \\ B_3^{(k)} &= \frac{1}{a_{12}^{(k)}} \sum_{j=k+1}^{N} a_{12}^{(j)} \left(j - k - \frac{1}{2} \right) \\ B_4^{(k)} &= 1 \\ B_5^{(k)} &= \frac{1}{a_{32}^{(k)}} \sum_{j=k+1}^{N} a_{32}^{(j)} \end{aligned} \tag{15}$$

Furthermore, from the interface traction continuity condition, we can conclude that λ_1 and λ_2 are constant through the laminate.

So far, we have determined the coefficients $A_i^{(k)}$ and $B_i^{(k)}$ of the stress functions. Therefore, the stress solutions for the kth ply in the boundary-layer region can be formulated as follows:

$$\begin{aligned} f^{0(k)}_{rr} &= A_2^{(k)}(\exp(-\lambda_1\lambda_2\eta) - \lambda_2 \exp(\lambda_1\eta)) \\ f^{0(k)}_{r\theta} &= A_3^{(k)} \exp(-\lambda_1\eta) \\ f^{0(k)}_{rz} &= (\rho + B_2^{(k)})(A_2^{(k)}\lambda_1\lambda_2)(\exp(-\lambda_1\lambda_2\eta) - \exp(-\lambda_1\eta)) \\ f^{0(k)}_{z\theta} &= (\rho + B_5^{(k)})A_3^{(k)}\lambda_1 \exp(-\lambda_1\eta) \\ f^{0(k)}_{zz} &= (\tfrac{1}{2}\rho^2 + B_2^{(k)}\rho + B_3^{(k)})(A_2^{(k)}\lambda_1^2\lambda_2)(\lambda_2 \exp(-\lambda_1\lambda_2\eta) \\ &\quad - \exp(-\lambda_1\eta)) \\ f^{0(k)}_{\theta\theta} &= -(\bar{S}_{12}^{(k)} f^{0(k)}_{rr} + \bar{S}_{23}^{(k)} f^{0(k)}_{zz} + \bar{S}_{26}^{(k)} f^{0(k)}_{r\theta})/\bar{S}_{22}^{(k)} \end{aligned} \tag{16}$$

where the $\bar{S}_{ij}^{(k)}$ are anisotropic compliances for the kth ply.

By superpositioning the stress solutions from the interior and boundary-layer regions, we can obtain the expressions for total stress components:

$$\begin{aligned} \sigma_{rr}^{(k)} &= \sigma_{rr}^{0(k)} + f_{rr}^{0(k)} \\ \sigma_{\theta\theta}^{(k)} &= \sigma_{\theta\theta}^{0(k)} + f_{\theta\theta}^{0(k)} \\ \tau_{r\theta}^{(k)} &= \tau_{r\theta}^{0(k)} + f_{r\theta}^{0(k)} \\ \tau_{rz}^{(k)} &= f_{rz}^{0(k)} \\ \tau_{z\theta}^{(k)} &= f_{z\theta}^{0(k)} \\ \sigma_{zz}^{(k)} &= f_{zz}^{0(k)} \end{aligned} \tag{17}$$

E. Complementary Energy Minimization

It is obvious that the problem is reduced to solve the unknown parameters λ_1 and λ_2 which are to be determined by complementary energy minimization for the zeroth order. In addition, the external work has no contribution to complementary energy minimization due to its independence with respect to λ_1 and λ_2.

$$\begin{aligned} \delta\Pi_c = \delta \Bigg\{ & \sum_{k=1}^{N} \frac{1}{2} \int_{-\pi}^{\pi} \int_0^1 \int_{0V^{(k)}}^{\infty} \\ & \times [(\hat{S}_{11} f^0_{rr} + \hat{S}_{13} f^0_{zz} + \hat{S}_{16} f^0_{r\theta}) f^0_{rr} \\ & + (\hat{S}_{13} f^0_{rr} + \hat{S}_{33} f^0_{zz} + \hat{S}_{36} f^0_{r\theta}) f^0_{zz} \\ & + (\hat{S}_{16} f^0_{rr} + \hat{S}_{36} f^0_{zz} + \hat{S}_{66} f^0_{r\theta}) f^0_{r\theta} \\ & + (\hat{S}_{44} f^0_{z\theta} + \hat{S}_{45} f^0_{rz}) f^0_{z\theta} + (\hat{S}_{45} f^0_{z\theta} + \hat{S}_{55} f^0_{rz}) f^0_{rz}] \\ & \times (R + t\eta) t^2 d\eta d\rho d\theta \Bigg\} = 0 \end{aligned} \tag{18}$$

where

$$\hat{S}_{ij}^{(k)} = \bar{S}_{ij}^{(k)} - \bar{S}_{2i}^{(k)} \bar{S}_{2j}^{(k)} / \bar{S}_{22}^{(k)}$$

Substitution of stress components in Eq. (16) into Eq. (18) and then differentiation with respect to λ_1 and λ_2, respec-

tively, yields the following nonlinear simultaneous algebraic equations:

$$\frac{\partial \Pi_c}{\partial \lambda_1} = \{\lambda_1^5 R(3\lambda_2^5 P_{33} + 3\lambda_2^4 P_{33}) + \lambda_1^4 t(2\lambda_2^4 P_{33}) + \lambda_1^3 R[\lambda_2^4(-2P_{13} - 2P_{36} + P_{44} + 2P_{45} + P_{55}) + \lambda_2^3(-2P_{13} - 2P_{36} + 2P_{44} + 2P_{45} + P_{55}) + \lambda_2^2 R P_{44}] - \lambda_1 R[\lambda_2^4(P_{11} + 2P_{16} + P_{66}) + \lambda_2^3(4P_{11} + 6P_{16} + 2P_{66}) + \lambda_2^2(4P_{11} + 4P_{16} + P_{66}) + \lambda_2 P_{11}] - t[\lambda_2^4(P_{11} + 2P_{16} + P_{66}) + \lambda_2^3(4P_{11} + 6P_{16} + 2P_{66}) + \lambda_2^2(8P_{11} + 8P_{16} + P_{66}) + 4\lambda_2 P_{11} + P_{11}]\} = 0 \quad (19)$$

$$\frac{\partial \Pi_c}{\partial \lambda_2} = \{\lambda_2^6 R(\lambda_1^5 P_{33}) + \lambda_2^5(3\lambda_1^5 P_{33}) + \lambda_2^4[2\lambda_1^5 R P_{33} + 2\lambda_1^4 t P_{33} + \lambda_1^3 R(-2P_{13} - 2P_{36} + 2P_{45} + P_{55}) - \lambda_1^2 t(-2P_{13} - 3P_{36} + P_{45} + P_{55}) - \lambda_1 R(2P_{11} + 2P_{16} - t(P_{11} + P_{16})] + \lambda_2^3[\lambda_1^3 R(-2P_{13} - 2P_{36} + 2P_{45} + P_{55}) + \lambda_1^2(-2P_{13} - P_{36} + 3P_{45} + P_{55}) - \lambda_1 R(4P_{11} + 2P_{16}) - t(6P_{11} + 5P_{16})] - \lambda_2^2(3\lambda_1 R P_{11} + 6tP_{11}) - \lambda_2(\lambda_1 R P_{11} + 4tP_{11}) - tP_{11}\} = 0 \quad (20)$$

where the coefficients P_{ij} are calculated by means of 32-point Gaussian quadrature formulas and given in the appendix.

Due to the complexity of the nonlinear simultaneous Eqs. (19) and (20), it is not easy to find the exact expression of solutions. Therefore, the employment of numerical technique such as Newton-Raphson iterative method is necessary. Normally, there are thirty pairs of λ_1 and λ_2 for Eqs. (19) and (20). However, only one pair that has positive real value and makes the complementary energy minimization is needed. A detail algorithm for solving λ_1 and λ_2 is given in Ref. 5 and followed in the present analysis. A recommended starting value for λ_1 is 1.0 (1/in.).

III. Numerical Results and Discussions

In order to check the accuracy and efficiency of the present method, comparisons of numerical results with literature are presented. The following material properties of a single ply for boron/epoxy used in the present study are given by Refs. 8 and 13–15, i.e., $E_{11} = 30.0$ Msi, $E_{22} = E_{33} = 3.0$ Msi, $G_{12} = G_{13} = G_{23} = 1.0$ Msi, $\nu_{12} = \nu_{13} = \nu_{23} = 0.336$. For the purpose of assessing the efficiency of this method, laminates of $(45/-45\ \text{deg})_S$ basis due to far-field uniaxial tension are considered. The values of decay parameters λ_1 and λ_2, computer execution time on a CDC 180/830 computer system, and the number of iterations are given in Table 1. It can be seen, from these results, that the current technique is very efficient even for laminates with numerous plies. It is also interesting to note that the magnitudes of λ_2 decrease with the increasing number of plies. This phenomenon reveals that the influence of the second exponential function in Eq. (10d) on the interlaminar normal stress declines for laminates with a number of plies.

The case of a $(90/0\ \text{deg})_S$ laminate subjected to uniaxial tension is considered. The circumferential stress distributions for 0-deg and 90-deg ply around the circular hole boundary (at $r = R$), by the present method, are compared with those by Tang[8] and Nishioka and Atluri[15] as shown in Fig. 3. It can be seen that they are in excellent agreement. The circumferential stress $\sigma_{\theta\theta}$ at $\theta = 90$ deg for 0-deg and 90-deg ply is approximately in the ratio of 10:1, which is nearly identical to the ratio of longitudinal modulus E_{11} to transverse modulus E_{22}. This result is not surprising from a structural viewpoint. As a matter of fact, the composite laminate in itself is a complex structure, therefore, the overall stress will be shared according to the relative stiffness of each ply. The variation of interlaminar shear stress $\tau_{z\theta}$ at 90/0 deg interface is shown in Fig. 4. It is seen that the present results have good agreement compared with those of Tang.[8] However, these results do not agree well with those of Rybicki and Hopper[13] except for the value and location of peak stress. This discrepancy may be attributed to the assumption of Rybicki and Hopper,[13] in which the in-plane stresses are assumed to be continuous along the ply interface. Fig. 5 shows the distributions of interlaminar normal stress σ_{zz} at the midplane of the laminate around the hole. It can be observed that the present results have a similar trend with those of Refs. 14 and 15 except for small angles. However, the discrepancy between the present results and those of Ref. 8 is considerable, especially at $\theta =$

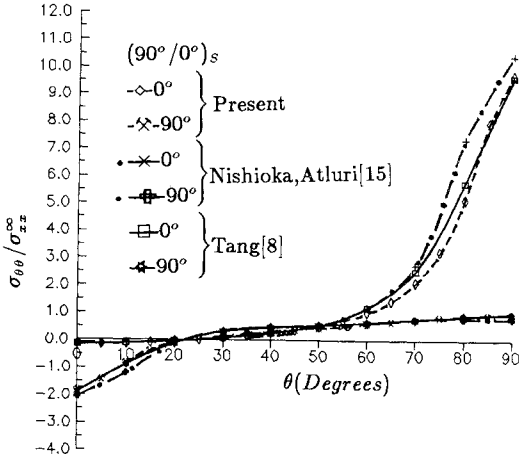

Fig. 3 Circumferential ply stress $\sigma_{\theta\theta}$ around a circular hole of a $(90/0\ \text{deg})_S$ laminate under uniaxial tension, $R/H = 1.25$.

Table 1 Computer execution time and number of iterations for various laminates

Laminate construction	R/H	CPU, s	Iteration no.	λ_1, 1/in.	λ_2
$(45/-45\ \text{deg})_S$	100.0	1.035	6	1.1483	1.1855
$(45/-45\ \text{deg})_{2S}$	50.0	1.532	7	1.1518	0.6664
$(45/-45\ \text{deg})_{4S}$	25.0	2.334	8	1.1532	0.3825
$(45/-45\ \text{deg})_{8S}$	12.5	4.350	9	1.1513	0.2273
$(45/-45\ \text{deg})_{12S}$	8.33	7.070	10	1.1481	0.1700
$(45/-45\ \text{deg})_{24S}$	4.17	19.046	11	1.1381	0.1055

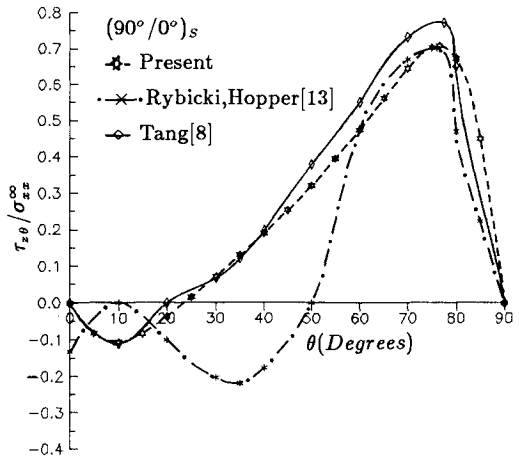

Fig. 4 Interlaminar shear stress $\tau_{z\theta}$ around a circular hole at 90/0-deg interface of a (90/0 deg)$_S$ laminate, R/H = 1.25.

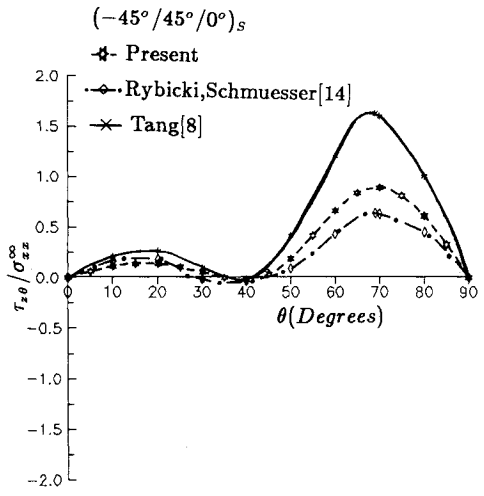

Fig. 6 Interlaminar shear stress $\tau_{z\theta}$ around a circular hole at 45/0-deg interface of a (−45/45/0 deg)$_S$ laminate, R/H = 100.

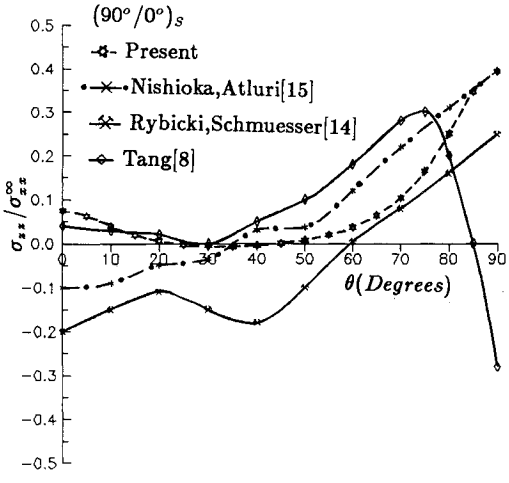

Fig. 5 Interlaminar normal stress σ_{zz} around a circular hole at the midplane of a (90/0 deg)$_S$ laminate, R/H = 1.25.

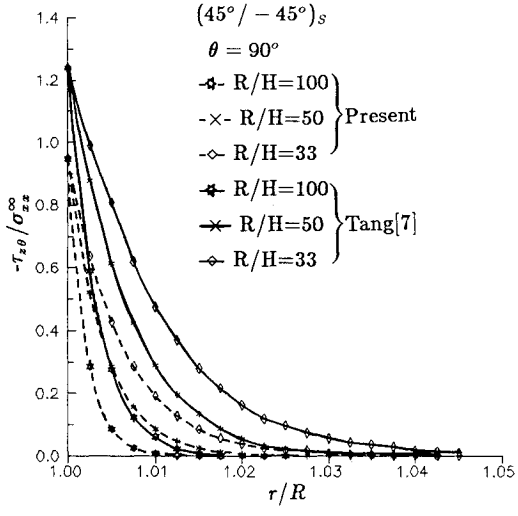

Fig. 7 Interlaminar shear stress $\tau_{z\theta}$ distributions from the hole edge for various R/H ratios.

90 deg. The main reason may be, as mentioned earlier, that the stress functions of Ref. 8 cannot satisfy all the boundary conditions exactly.

Furthermore, a (−45/45/0 deg)$_S$ angle-ply laminate subjected to uniaxial tension is analyzed. The variation of interlaminar shear stress $\tau_{z\theta}$ at 45/0 deg interface is shown in Fig. 6. It can be seen that there are excellent qualitative agreements between the present results and those of Tang[8] and Rybicki and Schmuesser,[14] however, the magnitudes are different. The curve, from the present results, lies between those of Refs. 8 and 14, and it is believed that the present results should be more reliable due to the exact satisfactions of all the traction-free-edge boundary conditions and interface traction continuity.

In order to have additional comparisons with the available results in the literature, other material properties for graphite/epoxy are introduced as follows: E_{11} = 20.0 Msi, $E_{22} = E_{33}$ = 2.1 Msi, $G_{12} = G_{13} = G_{23}$ = 0.85 Msi, $\nu_{12} = \nu_{13} = \nu_{23}$ = 0.21. The effect of the hole-radius-to-laiminate-thickness ratio R/H on the interlaminar shear stress at 45/−45-deg interface of a (45/−45 deg)$_S$ laminate due to uniaxial tension is shown in Fig. 7. It can be seen that the present results have a similar trend compared with those of Tang,[7] which reveals that the boundary-layer effect for a high R/H ratio or a thin laminate dissipates more quickly than a small R/H ratio or a thick laminate. In addition, it is worth noting that the decay parameter in Ref. 7 is equal to 0.785 (i.e., $\pi/2m$, 2m is the number of plies) which is independent on the material properties of the laminate. This point conflicts with the results presented in Refs. 3–5 and this paper.

The distribution of interlaminar shear stress $\tau_{z\theta}$ at 0/90 deg interface of a (0/90 deg)$_S$ laminate at θ = 45 deg vs the nondimensional radial coordinate $(r - R)/2H$ under far-field pure shear is shown in Fig. 8 along with the comparison results of Zhang and Ueng.[10] It can be seen that the present results agree well with those of Ref. 10 except along the hole boundary (at $r = R$). This discrepancy may be attributed to the assumed order of stress singularity of Zhang and Ueng.[10]

In order to understand the variation of interlaminar stresses due to different loading conditions, the case of a (90/0 deg)$_S$ boron/epoxy laminate, adopted in previous examples, subjected to two different loading conditions, namely, uniaxial tension and pure shear, is considered. The results for the variation of interlaminar shear stress $\tau_{z\theta}$ around the hole at 90/0-deg interface are given in Fig. 9. It can be seen that the peak values of $\tau_{z\theta}$ for uniaxial tension and pure shear are at angles of about θ = 76.5 deg and 45 deg, respectively, and the magnitude for uniaxial tension is about half of that pure

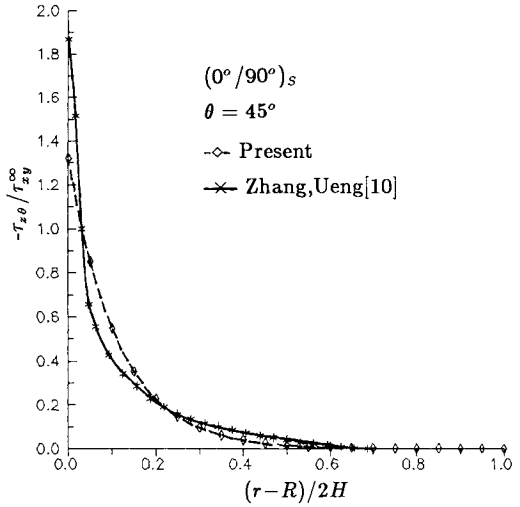

Fig. 8 Interlaminar shear stress $\tau_{z\theta}$ at 0/90-deg interface of a (0/90 deg)$_S$ laminate under pure shear.

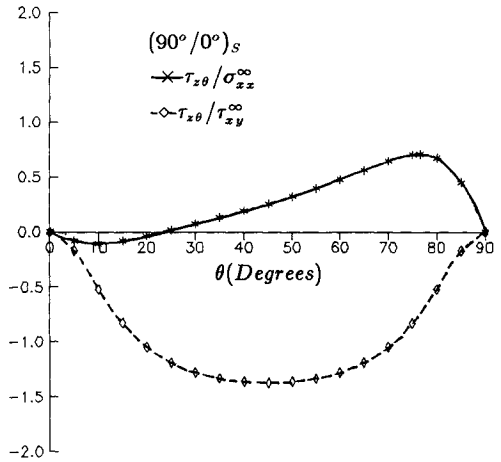

Fig. 9 Interlaminar shear stress $\tau_{z\theta}$ around a circular hole at 0/90-deg interface of a (90/0 deg)$_S$ laminate under various loading conditions, R/H = 1.25.

shear. It means that the interlaminar shear stress $\tau_{z\theta}$ caused by pure shear is more severe than that of uniaxial tension for (90/0 deg)$_S$ laminates.

The results for the variation of interlaminar normal stress σ_{zz} around the hole at the midplane for the same laminate are given in Fig. 10. Again, it can be seen that the peak values of σ_{zz} for uniaxial tension and pure shear are at angles of about θ = 90 deg and 12.5 deg individually and in a ratio about 1.23, which means the interlaminar normal stress σ_{zz} due to uniaxial tension is somewhat higher than pure shear. In addition, it is also interesting to see, from Figs. 9 and 10, that the distribution of interlaminar shear stress $\tau_{z\theta}$ is symmetric, while the interlaminar normal stress σ_{zz} is antisymmetric about the line of θ = 45 deg under the pure shear loading.

IV. Conclusions

An efficient analytical procedure to determine the three-dimensional stress distributions around a circular hole in symmetric laminates under a set of far-field stresses is presented. From the results obtained, the following conclusions can be reached:

1) The present solution needs less computation effort and computer execution time than any other method available in the literature. Moreover, solutions obtained are highly acceptable.

2) The accuracy of boundary-layer stresses distribution around the hole in composite laminates is highly dependent on the exact satisfaction of free-edge boundary conditions.

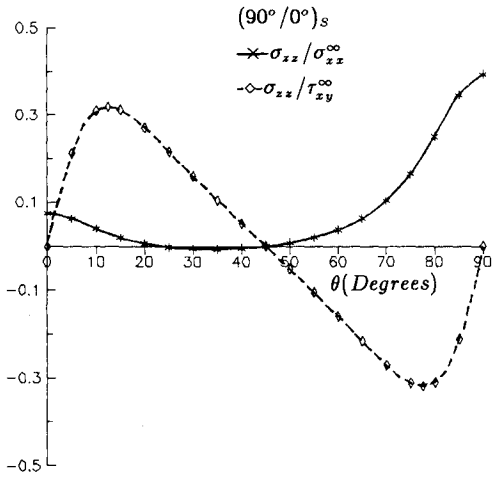

Fig. 10 Interlaminar normal stress σ_{zz} around a circular hole at the midplane of a (90/0 deg)$_S$ laminate under various loading conditions, R/H = 1.25.

3) The decay parameters for the boundary-layer stresses depend on the laminate properties and R/H ratio.

4) The boundary-layer effect for a high R/H ratio or a thin laminate dissipates more quickly than a small R/H ratio or a thick laminate.

5) The interlaminar shear stress $\tau_{z\theta}$ caused by pure shear is more severe than that of uniaxial tension, while the interlaminar normal stress σ_{zz} due to uniaxial tension is somewhat higher than pure shear for (90/0 deg)$_S$ laminates.

Appendix

Expressions for P_{ij} in Eqs. (19) and (20):

$$P_{11} = \sum_{k=1}^{N} \int_{-\pi}^{\pi} \hat{S}_{11}^{(k)} p_1^2 q \, d\theta$$

$$P_{13} = \sum_{k=1}^{N} \int_{-\pi}^{\pi} \hat{S}_{13}^{(k)} p_1^2 q (1/6 + 1/2B_2^{(k)} + B_3^{(k)}) \, d\theta$$

$$P_{16} = \sum_{k=1}^{N} \int_{-\pi}^{\pi} \hat{S}_{16}^{(k)} p_1 p_2 q \, d\theta$$

$$P_{33} = \sum_{k=1}^{N} \int_{-\pi}^{\pi} \hat{S}_{33}^{(k)} p_1^2 q [1/20 + (1/4B_2^{(k)} + 1/3B_2^{(k)^2}) + (1/3B_3^{(k)} + B_3^{(k)^2}) + B_2^{(k)} B_3^{(k)}] \, d\theta$$

$$P_{36} = \sum_{k=1}^{N} \int_{-\pi}^{\pi} \hat{S}_{36}^{(k)} p_1 p_2 q (1/6 + 1/2B_2^{(k)} + B_3^{(k)}) \, d\theta$$

$$P_{66} = \sum_{k=1}^{N} \int_{-\pi}^{\pi} \hat{S}_{66}^{(k)} p_2^2 q \, d\theta$$

$$P_{44} = \sum_{k=1}^{N} \int_{-\pi}^{\pi} \hat{S}_{44}^{(k)} p_2^2 q [1/3 + B_5^{(k)} + B_5^{(k)^2}) \, d\theta$$

$$P_{45} = \sum_{k=1}^{N} \int_{-\pi}^{\pi} \hat{S}_{45}^{(k)} p_1 p_2 q [1/3 + 1/2(B_2^{(k)} + B_5^{(k)}) + B_2^{(k)} B_5^{(k)}] \, d\theta$$

$$P_{55} = \sum_{k=1}^{N} \int_{-\pi}^{\pi} \hat{S}_{55}^{(k)} p_1^2 q [1/3 + B_2^{(k)} + B_2^{(k)^2}) \, d\theta$$

where $p_1 = a_{12}^{(k)}$, $p_2 = a_{32}^{(k)}$, $q = \sigma_{\theta\theta}^{o2}|_{\eta=0}$.

Acknowledgment

This paper is a part of the research work supported by a research grant from the National Science Council, Republic of China.

References

[1]Pipes, R. B., and Pagano, N. J., "Interlaminar Stresses in Composite Laminates Under Uniform Axial Extension," *Journal of Composite Materials*, Vol. 4, 1970, pp. 538–548.

[2]Wang, A. S. D., and Crossman, F. W., "Some New Results on Edge Effect in Symmetric Composite Laminates," *Journal of Composite Materials*, Vol. 11, 1977, pp. 92–106.

[3]Wang, S. S., and Choi, I., "Boundary-Layer Effect in Composite Laminates: Part 1. Free Edge Stress Singularities," *ASME Journal of Applied Mechanics*, Vol. 49, 1982, pp. 541–548.

[4]Wang, S. S., and Choi, I., "Boundary-Layer Effect in Composite Laminates: Part 2. Free Edge Stress Solutions and Basic Characteristics," *ASME Journal of Applied Mechanics*, Vol. 49, 1982, pp. 549–560.

[5]Kassapoglou, C., and Lagace, P. A., "An Efficient Method for the Calculation of Interlaminar Stresses in Composite Materials," *ASME Journal of Applied Mechanics*, Vol. 53, 1986, pp. 744–750.

[6]Reiss, E. L., "Extension of an Infinie Plate with a Circular Hole," *SIAM Journal*, Vol. 14, 1963, pp. 840–854.

[7]Tang, S., "Interlaminar Stresses Around Circular Cutouts in Composite Plates under Tension," *AIAA Journal*, Vol. 15, 1977, pp. 1631–1637.

[8]Tang, S., "A Variational Approach to Edge Stresses of Circular Cutout in Composites," *AIAA/ASME/ASCE/AHS, SDM Conf.*, St. Louis, MO, 1979, pp. 326–332.

[9]Spilker, R. L., and Chou, S. C., "Edge Effects in Symmetric Composite Laminates: Importance of Satisfying the Traction-Free-Edge Condition," *Journal of Composite Materials*, Vol. 14, 1980, pp. 2–20.

[10]Zhang, K. D., and Ueng, C. E. S., "A Simplified Approach for Interlaminar Stresses Around a Hole in $(0°/90°)_S$ Laminates," *Journal of Composite Materials*, Vol. 22, 1988, pp. 192–202.

[11]Rybicki, E. F., and Schmuesser, D. W., "Effect of Stacking Sequence and Lay-Up Angle on Free Edge Stresses Around a Hole in a Laminated Plate under Tension," *Journal of Composite Materials*, Vol. 12, 1978, pp. 300–313.

[12]Lucking, W. M., Hoa, S. V., and Sanker, T. S., "The Effect of Geometry on the Interlaminar Stresses of $(0°/90°)_S$ Composite Laminates with Circular Holes," *Journal of Composite Materials*, Vol. 17, 1984, pp. 188–198.

[13]Rybicki, E. F., and Hooper, A. T., "Analytical Investigation of Stress Concentrations due to Hole in Fiber Reinforced Plastic Laminated Plates, Three-Dimensional Models," Technical Rept. AFML-TR-73-100, Battelle Columbus Labs, 1973.

[14]Rybicki, E. F., and Schmuesser, D. W., "Three-Dimensional Finite Element Stress Analysis of Laminates Plates Containing a Circular Hole," Technical Rept. AFML-TR-76-92, Battelle Columbus Labs, 1976.

[15]Nishioka, T., and Atluri, S. N., "Stress Analysis of Holes in Angle-Ply Laminates: an Efficient Assumed Stress Special-Hole-Element Approach and a Simple Estimation Method," *Computers & Structures*, Vol. 15, 1982, pp. 135–147.

[16]Bar-Yoseph, P., and Avrashi, J., "Interlaminar Stress Analysis for Laminated Plates Containing a Curvilinear Hole," *Computers & Structures*, Vol. 21, 1985, pp. 917–932.

[17]Pagano, N. J., and Soni, S. R., "Global-Local Laminate Variational Model," *International Journal of Solids and Structures*, Vol. 19, 1983, pp. 207–228.

[18]Lekhnitskii, S. G., *Theory of Elasticity of an Anisotropic Body*, Holden Day, San Francisco, 1963, Ch. 4.

[19]Jones, R. M., *Mechanices of Composite Materials*, McGraw-Hill, New York, 1970, Ch. 4.

[20]System/360 Scientific Subroutine Package (SSP), Version III, IBM Corp., Technical Publication Dept., White Plains, NY, 1970, pp. 181–183.